Geomechanics and Engineering, *Vol. 9, No. 4 (2015) 499-511*
DOI: http://dx.doi.org/10.12989/gae.2015.9.4.499

An improved Maxwell creep model for salt rock

Jun-Bao Wang *[1,2], Xin-Rong Liu [1,2], Zhan-Ping Song [1] and Zhu-Shan Shao [1]

[1] *School of Civil Engineering, Xi'an University of Architecture and Technology, Xi'an, China*
[2] *School of Civil Engineering, Chongqing University, Chongqing, China*

(*Received March 09, 2015, Revised June 12, 2015, Accepted June 16, 2015*)

Abstract. The creep property of salt rock significantly influences the long-term stability of the salt rock underground storage. Triaxial creep tests were performed to investigate the creep behavior of salt rock. The test results indicate that the creep of salt rock has a nonlinear characteristic, which is related to stress level and creep time. The higher the stress level, the longer the creep time, the more obvious the nonlinear characteristic will be. The elastic modulus of salt rock decreases with the prolonged creep time, which shows that the creep damage is produced for the gradual expansion of internal cracks, defects, etc., causing degradation of mechanical properties; meanwhile, the creep rate of salt rock also decreases with the prolonged creep time in the primary creep stage, which indicates that the mechanical properties of salt rock are hardened and strengthened. That is to say, damage and hardening exist simultaneously during the creep of salt rock. Both the damage effect and the hardening effect are considered, an improved Maxwell creep model is proposed by connecting an elastic body softened over time with a viscosity body hardened over time in series, and the creep equation of which is deduced. Creep test data of salt rock are used to evaluate the reasonability and applicability of the improved Maxwell model. The fitting curves are in excellent agreement with the creep test data, and compared with the classical Burgers model, the improved Maxwell model is able to precisely predict the long-term creep deformation of salt rock, illustrating our model can perfectly describe the creep property of salt rock.

Keywords: salt rock; creep model; damage; hardening

1. Introduction

Salt rock has a number of advantages, including the compact structure, low porosity, low permeability, strong damage self-recovery capability, etc., which is internationally recognized as a suitable medium for underground storage of petroleum, natural gas, etc. and underground disposal of radioactive waste (Yang *et al*. 2013, Ozarslan 2012, Liang *et al*. 2011, Dethlefsen *et al*. 2014, Wang *et al*. 2013). As one of the most important mechanical properties of salt rock, creep property significantly influences the long-term stability, safety and availability of the salt rock underground storage (Deng *et al*. 2014, Xing *et al*. 2014). Therefore, the study on creep property of salt rock is of significance.

Dubey and Gairola (2008) studied the influence of structural anisotropy on creep of salt rock, and found that at lower stress creep the development of tensile crack arrays and shear crack arrays

*Corresponding author, Lecturer, E-mail: xajdwangjunbao@163.com

http://www.techno-press.org/?journal=gae&subpage=7 ISSN: 2005-307X (Print), 2092-6219 (Online)

was assisted by structural anisotropy, while at higher stress level creeps, the control of structural anisotropy on deformation became negligible. Zhang *et al*. (2012) conducted triaxial creep tests to the glauberite, anhydrite, and argillaceous rock salt, and found that the creep constitutive equations of different kinds of rock salt are in good agreement with the Burgers model. Rahimi and Hosseini (2014) conducted triaxial creep tests on thick-walled hollow cylindrical rock salt specimens, and developed a mathematical equation to estimate the strain rate in various stress fields. Zhou *et al*. (2013) constructed creep constitutive model by replacing a Newtonian dashpot in the classical Nishihara model with the fractional derivative Abel dashpot. Nazary Moghadama *et al*. (2013) utilized an elasto-viscoplastic constitutive model to describe dilatancy, short-term failure as well as long-term failure during transient and steady state creep of rock salt. Wang *et al*. (2014) studied the creep properties of salt rock under low-frequency cyclic loading, and established creep damage model for salt rock. Wu *et al*. (2015) proposed a new method of building creep model for salt rock based on variable-order fractional derivatives. The order of the fractional derivative is allowed to be a function of time, rather than a constant of arbitrary order. Fuenkajorn and Phueakphum (2010) performed a series of laboratory testing to assess the effects of cyclic loading on compressive strength, elasticity and time-dependency of salt rock, and found that the compressive strength decreases with increasing number of loading cycles, which can be best represented by a power equation. Combined with the generalized Hoek-Brown model, Ma *et al*. (2013) formulated a three-dimensional creep damage constitutive model, which enables both the three creep phases and the deformation induced by vicious damage and plastic flow to be calculated. Özşen *et al*. (2014) conducted creep tests on the Tuzköy salt rock, and proposed a mathematical model which determines the total creep process as well as the first, second and third creep stages separately to explain the creep behaviour of salt rock. By introducing the concept of "damage accelerating limit" into Carter's creep model, a new constitutive creep-damage model for salt rock was established by Wang (2004). Chan *et al*. (1997) proposed a Multimechanism Deformation Coupled Fracture (MDCF) model for salt rock by incorporating continuum, isotropic damage as a fully coupled variable that enhanced the stress influence by reduction of the effective area and contributed directly to the inelastic strain rate. In this MDCF model, the mechanisms of dislocation creep, shear creep, tensile damage, damage healing etc can be considered. However, because this model is quite complex and more than 30 parameters need to be determined, it is not convenient to use.

Generally, the creep models for salt rock can be classified into 3 types, namely empirical models, component models and damage models. The empirical models are empirical expressions built on test results, with advantages of simple equations and only several parameters. However, predicting the long-term deformation of salt rock with the empirical models tends to produce large errors, for these models cannot reflect the creep mechanical mechanism of salt rock but purely fitting mathematically. The component models are constructed through connecting the components with basic functions (including elastic component, plastic component and viscosity component, etc.) in series and parallel. These models can intuitively show the complicated mechanical properties of salt rock, and the parameters of which have explicit physical meanings. Nonetheless, as linear models, the component creep models cannot describe the nonlinearity of salt rock; therefore, in most cases, the theoretical results from these models are not in good agreement with the test data. The damage models serve as relatively ideal models, starting with the evolutionary of tiny microcosmic defect inside the materials with time, taking the change of internal structure into consideration and overcoming the disadvantage of empirical models and component models that they only consider the macroscopic phenomenological behavior. However, during the creep of salt rock, besides the degrading mechanical properties caused by expanding damage, the creep rate decreases gradually with time in primary creep stage, which indicates that the mechanical properties of salt rock are hardened and strengthened. For this, damage and hardening exist simultaneously during the creep of salt rock.

In order to precisely predict the long-term deformation behavior of salt rock, based on the analysis of salt rock creep test results, an improved Maxwell creep model is proposed by considering the degrading elastic modulus and hardening viscosity coefficient during creep, and the reasonability and applicability of the model are verified in this study.

2. Creep test results

Salt rock sample used in the test was obtained from a salt mine in Huai'an, Jiangsu, China, with a natural density of about 2.2 g/cm^3. The sample was prepared as a cylinder with a diameter of 50 mm and a height of 100 mm, according to the International Society for Rock Mechanics (Hatheway 2009).

The sample is loaded in a manner of echelonment during the creep test, namely applying the axial stress step by step on the same sample in ascending order under the circumstance that the confining pressure (σ_3) is not changed, which is set to 15MPa. In order to avoid the influence of ambient change on test results, the indoor temperature is kept at 25 ± 1°C during the test.

When confining pressure (σ_3) is 15MPa, the triaxial strength (σ_0) of the salt rock is 94MPa (Wang 2012). As the range of the deformation sensor of the rheology testing machine adopted in this test has its limitations and salt rock has strong deformation ability, the axial stress levels applied on the sample are relatively low. Otherwise, it may be caused that the creep deformation of salt rock exceeds the effective measuring range of the testing machine. Based on the aforesaid analysis, the axial stress levels applied on the salt rock sample in this creep test are determined as 20 MPa ($0.21\sigma_0$), 25 MPa ($0.27\sigma_0$) and 30 MPa ($0.32\sigma_0$) respectively.

Fig. 1 shows the obtained axial creep curves of salt rock under three different axial stress levels. The values (in MPa) in Fig. 1 represent the axial stress level. It can be seen from Fig. 1 that the deformation of salt rock is composed of the instant deformation generated during loading process and the creep deformation increasing with time; the creep of salt rock goes through primary creep stage and steady creep stage in test duration; the creep rate of salt rock (the slope of the creep

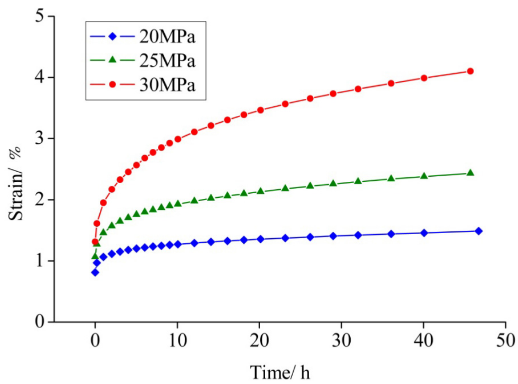

Fig. 1 Axial creep curves of salt rock

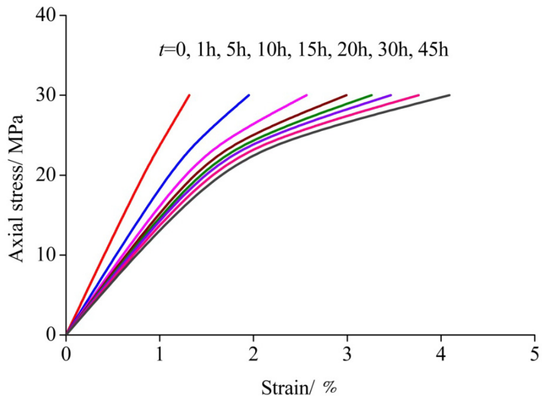

Fig. 2 Isochronous stress-strain curves of salt rock

curves) decreases with time in primary creep stage, and mainly remains unchanged in steady creep stage; the instant deformation, creep deformation at the same time and steady creep rate of salt rock are all increased with the increase in values of axial stress level.

The isochronous stress-strain curves of salt rock can be plotted according to the creep test data in Fig. 1, as shown in Fig. 2. From Fig. 2, we can see that the stress-strain curve approximates a straight line when time is 0, so we can deem that the instant deformation of salt rock is mainly the elastic deformation. When time is not 0, it has an obvious inflection point from a straight line to a curved line for an arbitrary stress-strain curve; that is to say, the stress-strain curve actually a straight line when axial stress level is relatively low; with the increase of stress level, it increasingly bends to the strain axis. In addition, the stress-strain curve bends to the strain axis more obviously and the slope of which gradually decreases with the prolonged creep time. This indicates that the creep of salt rock has a nonlinear characteristic, which is related to stress level and creep time. The higher the stress level, the longer the creep time, the more obvious the nonlinear characteristic will be. This is similar to the observations from Dubey and Gairola (2005).

See Fig. 3 for the variation in elastic modulus of salt rock (namely the slope of the straight line of isochronous stress-strain curve under a relatively low stress level in Fig. 2) with respect to time

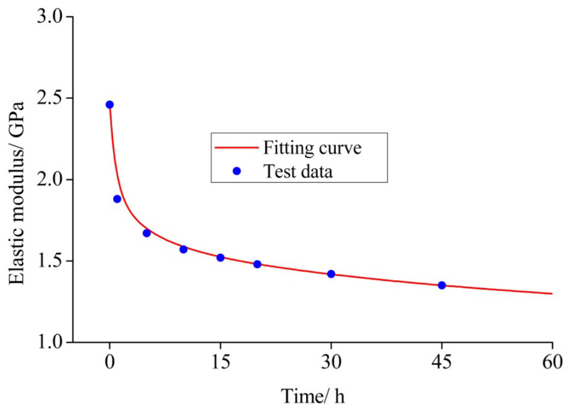

Fig. 3 Variation in elastic modulus with respect to time

when the confining pressure is 15MPa. As shown in Fig. 3, the elastic modulus of salt rock decreases rapidly with the elapse of time at the beginning of the test; with the continuous elapse of time, though the elastic modulus continues to decrease, the variation rate is lower and lower.

Through careful analysis, the variation in rock elastic modulus with respect to time can be described with the following exponential function

$$E_{\mathrm{T}}(t) = E_{\mathrm{T0}} \exp(-at^{n}) \tag{1}$$

where t is the time, $E_{\mathrm{T}}(t)$ is the elastic modulus at the moment of t, E_{T0} is the initial elastic modulus, and a and n are the fitting parameters.

As can be seen from Eq. (1), $E_{\mathrm{T}}(t) = E_{\mathrm{T0}}$ when $t = 0$, and $E_{\mathrm{T}}(\infty) = 0$ when $t \to \infty$. In addition, it can be demonstrated that Eq. (1) has monotonicity. Fitting analysis is made to the test data shown in Fig. 3 using Eq. (1), the parameters can be determined as E_{T0} = 2.461 GPa, a = 0.275 and n = 0.206. Fig. 3 simultaneously shows the comparison of test data and fitting curve. From the comparison, we can see that Eq. (1) is able to preferably describe the variation in elastic modulus with respect to time.

3. Creep model for salt rock

As analyzed in the previous section, the elastic modulus of salt rock is continuously decreasing with the prolonged time under the action of load during creep, which indicates that the creep damage has been produced for the gradual expansion of internal cracks, defects, etc., causing degradation of mechanical properties and increase of creep deformation. Therefore, the damage effect during the creep of salt rock can be described with the degradation of elastic modulus.

However, it is not adequate to consider the creep damage of salt rock only, because the mechanical properties of salt rock are constantly degrading with the gradual expansion of damage, and the creep rate should have been continuously increasing, but this is not the truth. From the creep curves of salt rock under different stress levels shown in Fig. 1, we can see that the creep rate of salt rock (the slope of the creep curves) is gradually decreasing with time, and can approximate a constant value only when creep time increases to a certain extent. This indicates that the mechanical properties of salt rock are hardened and strengthened in the primary creep stage, causing decrease of creep rate.

Therefore, damage and hardening exist simultaneously during the creep of salt rock, and they compete with each other. On the one hand, creep deformation will cause the expansion of internal existing cracks and the generation of new cracks, which leads to damage evolution and degradation of mechanical properties of salt rock; on the other hand, creep deformation will cause the deactivation of internal crack tip, ease the stress field near the crack tip, delay the crack growth and thus harden and strengthen the mechanical properties of salt rock, which are macroscopically shown as the decrease in values of creep rate (Fan and Gao 2007).

Viscosity coefficient is an important physical parameter to describe the fluidity of materials, defined by the ratio of stress and strain rate. So, the creep rate of materials can be represented with the viscosity coefficient of the viscosity body in component combination creep models. With this thought as reference, the variation in creep rate of salt rock with respect to time may be described with a viscosity body which is gradually hardened over time. We assume that the variation in viscosity coefficient of this viscosity body with respect to time conforms with the following equation.

$$\eta(t) = \eta_0 \frac{(b+ct)^2}{(b+ct)^2+1} \tag{2}$$

where $\eta(t)$ is the viscosity coefficient at the moment of t, and η_0, b and c are all the material parameters.

The characteristics of Eq. (2) are analyzed as follows.

Based on Eq. (2), when $t = 0$, we have

$$\eta(0) = \eta_0 \frac{b^2}{b^2+1} \neq 0 \tag{3}$$

This shows the initial value of $\eta(t)$ is not 0.

Taking the derivative with respect to t in Eq. (2) to get

$$\eta'(t) = \frac{2\eta_0 c(b+ct)}{\left[(b+ct)^2+1\right]^2} > 0 \tag{4}$$

This indicates that Eq. (2) increases monotonically.

Eq. (2) can be rewritten as

$$\eta(t) = \frac{\eta_0}{1+\dfrac{1}{(b+ct)^2}} \tag{5}$$

Eq. (5) shows that $\eta(\infty) = \eta_0$ when $t \to \infty$. Therefore, Eq. (2) has its maximum value of η_0.

It is clear that $\eta(t)$ increases monotonically from $\eta_0 b^2/(b^2+1)$ to η_0 when t increases from 0 to ∞. Theoretically, $\eta(t)$ can reach η_0 only when $t \to \infty$. However, because the parameters b and c are both constants, $1/(b+ct)^2$ approximates 0 when t increases to a certain extent, then $\eta(t)$ has approximated its maximum value of η_0.

Under the condition of constant stress, the viscosity coefficient of materials gradually increases with time, which will cause the decrease of creep rate. Therefore, the hardening effect of the mechanical properties of salt rock can be represented with the increase of viscosity coefficient.

The Maxwell creep model is comprised by connecting an elastic body with a viscosity body in series, as is shown in Fig. 4. Part I in Fig. 4 shows the elastic body (H body) and Party II, the viscosity body (N body). In addition, E and η represent elastic modulus and viscosity coefficient, respectively.

Under three-dimensional stress state, the stress tensor σ_{ij} at a certain point inside salt rock can be decomposed into the deviatoric stress tensor S_{ij} and the spherical stress tensor σ_{m}. Similarly, the strain tensor ε_{ij} can be decomposed into the deviatoric strain tensor e_{ij} and the spherical strain tensor ε_{m}.

The relationship of S_{ij}, σ_m and σ_{ij} can be expressed as

$$\begin{cases} S_{ij} = \sigma_{ij} - \delta_{ij}\sigma_{\mathrm{m}} \\ \sigma_{\mathrm{m}} = \dfrac{\sigma_1+\sigma_2+\sigma_3}{3} \end{cases} \tag{6}$$

where δ_{ij} is the Kronecker function, and σ_1, σ_2 and σ_3 are principal stresses in three directions

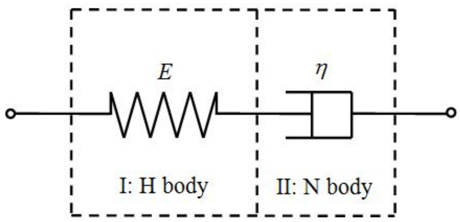

Fig. 4 Maxwell creep model under one-dimensional stress state

respectively.

The relationship of e_{ij}, ε_{m} and ε_{ij} can be expressed as

$$\begin{cases} e_{ij} = \varepsilon_{ij} - \delta_{ij}\varepsilon_{\mathrm{m}} \\ \varepsilon_{\mathrm{m}} = \dfrac{\varepsilon_1 + \varepsilon_2 + \varepsilon_3}{3} \end{cases} \tag{7}$$

where ε_1, ε_2 and ε_3 are principal strains in three directions respectively.

It is generally recognized that the spherical stress tensor can only change the bulk of the material, while the deviatoric stress tensor can only change its shape. Hence, it may be considered that the creep deformation of salt rock is only caused by the deviatoric stress tensor (Wang *et al*. 2014).

For the Maxwell creep model, because the two bodies are connected in series, there is

$$\begin{cases} S_{ij} = S_{\mathrm{H}ij} = S_{\mathrm{N}ij} \\ e_{ij} = e_{\mathrm{H}ij} + e_{\mathrm{N}ij} \end{cases} \tag{8}$$

where S_{ij} and e_{ij} are the total deviatoric stress tensor and total deviatoric strain tensor of the Maxwell model, $S_{\mathrm{H}ij}$ and $e_{\mathrm{H}ij}$ are the deviatoric stress tensor and deviatoric strain tensor of the elastic body, and $S_{\mathrm{N}ij}$ and $e_{\mathrm{N}ij}$ are the deviatoric stress tensor and deviatoric strain tensor of the viscosity body.

For the elastic body, according to the generalized Hooke's law, its constitutive relation is given by

$$\begin{cases} \sigma_{\mathrm{m}} = 3K\varepsilon_{\mathrm{m}} \\ S_{\mathrm{H}ij} = 2Ge_{\mathrm{H}ij} \end{cases} \tag{9}$$

where K is the bulk modulus, and G is the shear modulus, with

$$\begin{cases} K = \dfrac{E}{3(1-2\upsilon)} \\ G = \dfrac{E}{2(1+\upsilon)} \end{cases} \tag{10}$$

where υ is the Poisson's ratio.

Based on Eqs. (7) and (9), the strain tensor $\varepsilon_{\mathrm{H}ij}$ of the elastic body can be written as

$$\varepsilon_{\mathrm{H}ij} = \frac{S_{\mathrm{H}ij}}{2G} + \frac{\sigma_{\mathrm{m}}}{3K} \tag{11}$$

Substituting Eq. (10) into Eq. (11), we get

$$\varepsilon_{\mathrm{H}ij} = \frac{S_{\mathrm{H}ij}(1+\upsilon) + \sigma_{\mathrm{m}}(1-2\upsilon)}{E} \tag{12}$$

Eq. (12) is the final expression of the strain tensor of the conventional elastic body.

Here, an improved (softened) elastic body is proposed by introducing the damage effect to the conventional elastic body. Based on the creep test results, the elastic modulus of salt rock (E_{T}) under three-dimensional stress state continuously decreases with the prolonged time, which can be described with Eq. (1). We assume that the variation in elastic modulus of salt rock (E) under one-dimensional stress state with respect to time conforms with Eq. (1), too. Then, substituting Eq. (1) into Eq. (12), we can obtain the strain tensor of the improved elastic body as

$$\varepsilon_{\mathrm{H}ij} = \frac{S_{\mathrm{H}ij}(1+\upsilon) + \sigma_{\mathrm{m}}(1-2\upsilon)}{E_0 \exp(-at^n)} \tag{13}$$

For the viscosity body, its constitutive equation is given by

$$S_{\mathrm{N}ij} = 2\eta \frac{\mathrm{d}e_{\mathrm{N}ij}}{\mathrm{d}t} \tag{14}$$

To describe the creep behavior of salt rock accurately, an improved (hardened) viscosity body is proposed here by introducing the hardening effect to the conventional viscosity body. It is assumed that the variation in viscosity coefficient with respect to time conforms with Eq. (2). Then, substituting Eq. (2) into Eq. (14), we get the constitutive equation of the improved viscosity body as

$$S_{\mathrm{N}ij} = 2\eta_0 \frac{(b+ct)^2}{(b+ct)^2 + b} \frac{\mathrm{d}e_{\mathrm{N}ij}}{\mathrm{d}t} \tag{15}$$

Taking the integral with respect to t in Eq. (15) and considering the initial condition $e_{\mathrm{N}ij} = 0$ when $t = 0$, the deviatoric strain tensor of the improved viscosity body can be determined as

$$e_{\mathrm{N}ij} = \frac{S_{\mathrm{N}ij}}{2\eta_0} t \left(1 + \frac{1}{b+ct}\right) \tag{16}$$

Replacing the conventional elastic body and viscosity body in Maxwell model (Fig.4) with the improved (softened) elastic body and improved (hardened) viscosity body respectively, an improved Maxwell model can be constructed.

Combining Eqs. (7), (13) and (16), the strain tensor of this improved Maxwell model can be obtained as

$$\varepsilon_{ij} = \frac{S_{\mathrm{H}ij}(1+\upsilon) + \sigma_{\mathrm{m}}(1-2\upsilon)}{E_0 \exp(-at^n)} + \frac{S_{\mathrm{N}ij}}{2\eta_0} t \left(1 + \frac{1}{b+ct}\right) \tag{17}$$

For the conventional triaxial compression test, because of $\sigma_2 = \sigma_3$, according to Eq. (6), the axial deviatoric stress of the improved Maxwell model can be expressed as

$$S_{11} = \sigma_1 - \frac{\sigma_1 + 2\sigma_3}{3} = \frac{2(\sigma_1 - \sigma_3)}{3} = S_{\mathrm{H}11} = S_{\mathrm{N}11} \tag{18}$$

Substituting Eq. (18) into Eq. (17), the axial creep equation of the improved Maxwell model under three-dimensional stress state can be determined as

$$\varepsilon = \frac{2(1+\upsilon)(\sigma_1 - \sigma_3) + (1-2\upsilon)(\sigma_1 + 2\sigma_3)}{3E_0 \exp(-at^n)} + \frac{\sigma_1 - \sigma_3}{3\eta_0} t\left(1 + \frac{1}{b+ct}\right) \tag{19}$$

4. Model verification

Triaxial creep test data of salt rock shown in Fig. 1 are used to evaluate the reasonability and applicability of the improved Maxwell model proposed in this paper. Firstly, such 6 creep parameters as E_0, η_0, a, b, c and n in Eq. (19) need to be determined, and the Poisson's ratio of salt rock υ = 0.3 (Wang *et al*. 2014). These creep parameters are inversed using the curve-fitting method and 1stOpt mathematical optimization software based on the nonlinear least-squares theory. The fitting method and steps are as follows:

(I) Compile Eq. (19) into the fitting code which can be identified by the software in the form of self-defining function.

(II) Take the creep parameters to be inversed as the design variable, namely

$$\boldsymbol{X} = \{E_0, \eta_0, a, b, c, n\} \tag{20}$$

(III) Construct the following target function

$$Q = \sum_{i=1}^{N} \left[w_i(\boldsymbol{X}, t_i) - w_i\right]^2 \tag{21}$$

where N is the number of test data pairs, $W_i(\boldsymbol{X}, t_i)$ is the calculated strain value at the moment of t_i, w_i is the measured strain value in the test at the moment of t_i, and Q is the target function, namely the error-squared sum.

(IV) Set up the control precision of the target function Q and carry out the iteration solution. If the value of Q satisfies the precision requirement, iteration ceases and the calculated results are outputted; if not, iteration continues till the precision requirement is satisfied.

Table 1 lists the inversion results of creep parameters; Fig. 5 shows the comparison of fitting curves and test data. The values (in MPa) in Fig. 5 represent the axial stress level. From Table 1 and Fig. 5, we can see that the errors are very small and the fitting curves are in excellent agreement with the test data. Thus, our improved Maxwell model can perfectly describe the creep property of salt rock.

The final target of establishing creep model is to predict the long-term deformation of salt rock when the creep parameters have been gained. In order to evaluate the advantages of the improved Maxwell model in prediction long-term deformation of salt rock, the uniaxial creep test data of salt

Table 1 Creep parameters of salt rock

Axial stress/ MPa	E_0/ MPa	η_0/ MPa·h	a	b	c	n	Q
20	1 356	163 564	0.22	0.012	0.009	0.21	9.4×10^{-10}
25	1 503	155 685	0.25	0.021	0.007	0.25	1.4×10^{-8}
30	1 603	168 816	0.29	0.016	0.003	0.27	1.8×10^{-7}

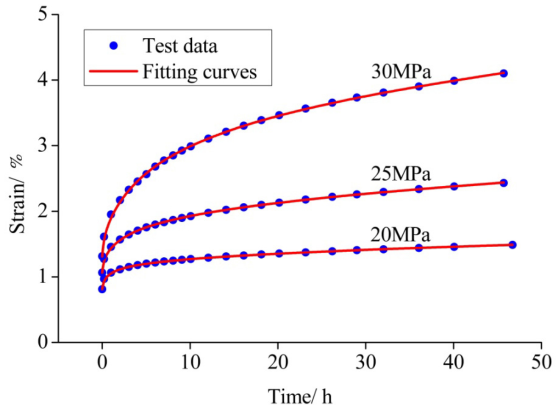

Fig. 5 Comparison of fitting curves and test data

rock (Hou 1997) are utilized to illustrate it. The test conditions are as follows: axial stress — 14.1 MPa; duration — 1256 days, about 3.44a; and laboratory temperature — 22°C. The creep test data are shown in Fig. 6.

As comparison of prediction effect, the creep test data within 1.14a in Fig. 6 (the first 11 data points) are used to inverse the creep parameters of the improved Maxwell model and the classical Burgers model respectively, while the creep test data after 1.14a are used to verify the prediction effect of these two models. The axial creep equation of the classical Burgers model (Yang *et al*. 2015) is given by

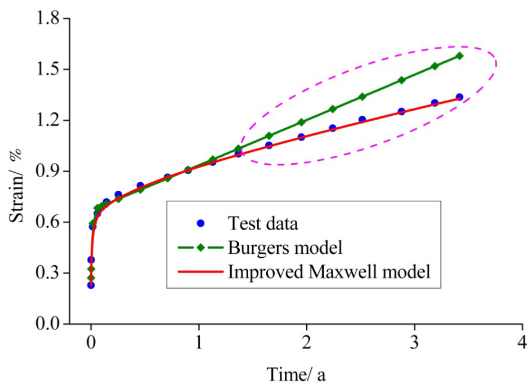

Fig. 6 Comparison of prediction curves and test data

$$\varepsilon = \frac{2(1+\upsilon)(\sigma_1 - \sigma_3) + (1-2\upsilon)(\sigma_1 + 2\sigma_3)}{3E} + \frac{\sigma_1 - \sigma_3}{3G_1}\left[1 - \exp\left(-\frac{G_1}{\eta_1}t\right)\right] + \frac{\sigma_1 - \sigma_3}{3\eta_2}t \tag{22}$$

The creep parameters of these two models are determined as follows: improved Maxwell model, E_0 = 6175 MPa, η_0 = 4370 MPa·a, a = 0.9, b = 0.002, c = 0.415, and n = 0.18; classical Burgers model, E = 5187 MPa, G_1 = 1184 MPa, η_1 = 12 MPa·a, and η_2 = 1763 MPa·a.

See Fig. 6 for the comparison of prediction curves and test data. As shown in Fig. 6, the prediction curve from the classical Burgers model has a good agreement with the test data only within 1.14a, while the difference between them becomes larger and larger with time increasing after 1.14a, as shown in the elliptical region in Fig. 6; however, the prediction curve from the improved Maxwell model favorably fits the test data from the beginning to the end. This indicates that the improved Maxwell model can also precisely predict the long-term deformation of salt rock even if the test duration is relatively short. Compared with the classical Burgers model, this model has obvious advantages in predicting long-term deformation of salt rock.

5. Conclusions

- The instant deformation, creep deformation at the same time and steady creep rate of salt rock all increase with the increase in values of axial stress level under the same confining pressure. The creep of salt rock has a nonlinear characteristic, which is related to stress level and creep time. The higher the stress level, the longer the creep time, the more obvious the nonlinear characteristic will be.
- The elastic modulus of salt rock decreases with the prolonged creep time, which shows that the creep damage is produced for the gradual expansion of internal cracks, defects, etc., causing degradation of mechanical properties; meanwhile, the creep rate of salt rock also decreases with the prolonged creep time in the primary creep stage, which indicates that the mechanical properties of salt rock are hardened and strengthened. That is to say, damage and hardening exist simultaneously during the creep of salt rock.
- Both the damage effect and the hardening effect are considered, an improved Maxwell creep model is proposed by connecting an elastic body softened over time with a viscosity body hardened over time in series, and the creep equation of which is deduced.
- Creep test data of salt rock are used to evaluate the reasonability and applicability of the improved Maxwell model. The fitting curves are in excellent agreement with the creep test data, and compared with the classical Burgers model, the improved Maxwell model is able to precisely predict the long-term creep deformation of salt rock. This shows that our model can perfectly describe the creep property of salt rock.

Acknowledgments

The present work is subsidized and supported by the National Natural Science Foundation of China (51404184) and the Specialized Scientific Research Program of Education Department of Shaanxi Provincial Government (14JK1401, 11JK0889). The financial supports are gratefully acknowledged by the authors!

References

Chan, K.S., Bodner, S.R., Fossum, A.F. and Munson, D.E. (1997), "A damage mechanics treatment of creep failure in rock salt", *Int. J. Damage Mech.*, **6**(2), 121-152.

Deng, J.Q., Yang, Q. and Liu, Y.R. (2014), "Time-dependent behaviour and stability evaluation of gas storage caverns in salt rock based on deformation reinforcement theory", *Tunn. Undergr. Sp. Tech.*, **42**, 277-292.

Dethlefsen, F., Ebert, M. and Dahmke, A. (2014), "A geological database for parameterization in numerical modeling of subsurface storage in northern Germany", *Environ. Earth Sci.*, **71**(5), 2227-2244.

Dubey, R.K. and Gairola, V.K., (2005), "Influence of stress rate on rheology-An experimental study on rock salt of Simla Himalaya, India", *Int. J. Geotech. Geol. Eng.*, **23**(6), 757-772.

Dubey, R.K. and Gairola, V.K. (2008), "Influence of structural anisotropy on creep of rock salt from Simla Himalaya, India: An experimental approach", *J. Struct. Geol.*, **30**(6), 710-718.

Fan, Q.Z. and Gao, Y.F. (2007), "Study on creep properties and nonlinear creep model of soft rock", *Chinese J. Rock Mech. Eng.*, **26**(2), 391-396. [In Chinese]

Fuenkajorn, K. and Phueakphum, D. (2010), "Effects of cyclic loading on mechanical properties of Maha Sarakham salt", *Eng. Geol.*, **112**(1), 43-52.

Hatheway, A.W. (2009), "The complete ISRM suggested methods for rock characterization, testing and monitoring: 1974-2006", *Environ. Eng. Geosci.*, **15**(1), 47-48.

Hou, Z. (1997), "Untersuchungen zum nachweis der standsicherheit fur untertagedeponien im salzgebirge", Ph. D. Dissertation; Technical University of Clausthal, Clausthal. [In German]

Liang, W.G., Zhao, Y.S., Xu, S.G. and Dusseault, M.B. (2011), "Effect of strain rate on the mechanical properties of salt rock", *Int. J. Rock Mech. Min. Sci.*, **48**(1), 161-167.

Ma, L.J., Liu, X.Y., Fang, Q., Xu, H.F., Xia, H.M., Li, E.B., Yang, S.G. and Li, W.P. (2013), "A new elasto-viscoplastic damage model combined with the generalized Hoek-Brown failure criterion for bedded rock salt and its application", *Rock Mech. Rock Eng.*, **46**(1), 53-66.

Nazary Moghadama, S., Mirzabozorg, H. and Noorzad, A. (2013), "Modeling time-dependent behavior of gas caverns in rock salt considering creep, dilatancy and failure", *Tunn. Undergr. Sp. Tech.*, **33**, 171-185.

Ozarslan, A. (2012), "Large-scale hydrogen energy storage in salt caverns", *Int. J. Hydrogen Energ.*, **37**(19), 14265- 14277.

Özşen, H., Özkan, İ. and Şensöğüt, C. (2014), "Measurement and mathematical modelling of the creep behaviour of Tuzköy rock salt", *Int. J. Rock Mech. Min. Sci.*, **66**(2), 128-135.

Rahimi, S. and Hosseini, M. (2014), "Laboratory studies of creep behavior on thick-walled hollow cylindrical salt rock specimens", *Arab. J. Geosci.*, **8**(8), 5949-5957. DOI: 10.1007/s12517-014-1622-5.

Wang, G.J. (2004), "A new constitutive creep-damage model for salt rock and its characteristics", *Int. J. Rock Mech. Min. Sci.*, **41**(Supp.1), 61-67.

Wang, J.B. (2012), "Study on the creep mechanical properties of salt rock under different loading paths and long-term stability of salt rock gas storage", Ph.D. Dissertation; Chongqing University, Chongqing, China. [In Chinese]

Wang, T.T., Yan, X.Z., Yang, H.L., Yang, X.J., Jiang, T.T. and Zhao, S. (2013), "A new shape design method of salt cavern used as underground gas storage", *Appl. Energ.*, **104**, 50-61.

Wang, J.B., Liu, X.R., Liu, X.J. and Huang, M. (2014), "Creep properties and damage model for salt rock under low-frequency cyclic loading", *Geomech. Eng., Int. J.*, **7**(5), 569-587.

Wu, F., Liu, J.F. and Wang, J. (2015), "An improved Maxwell creep model for rock based on variable-order fractional derivatives", *Environ. Earth Sci.*, **73**(11), 6965-6971. DOI: 10.1007/s12665-015-4137-9.

Xing, W., Zhao, J., Düsterloh, U., Brückner, D., Hou, Z.M., Xie, L.Z. and Liu, J.F. (2014), "Experimental study of mechanical and hydraulic properties of bedded rock salt from the Jintan location", *Acta Geotech.*, **9**(1), 145-151.

Yang, C.H., Jing, W.J., Daemen, J.J.K., Zhang, G.M. and Du, C. (2013), "Analysis of major risks associated

with hydrocarbon storage caverns in bedded salt rock", *Reliab. Eng. Syst. Safe.*, **113**, 94-111.
Yang, S.Q., Xu, P., Ranjith, P.G., Chen, G.F. and Jing, H.W. (2015), "Evaluation of creep mechanical behavior of deep-buried marble under triaxial cyclic loading", *Arab. J. Geosci.*, **8**(9), 6567-6582. DOI: 10.1007/s12517-014- 1708-0.
Zhang, H.B., Wang, Z.Y., Zheng, Y.L., Duan, P.J. and Ding, S.L. (2012), "Study on triaxial creep experiment and constitutive relation of different rock salt", *Safety Sci.*, **50**(4), 801-805.
Zhou, H.W., Wang, C.P., Mishnaevsky, Jr. L., Duan, Z.Q. and Ding, J.Y. (2013), "A fractional derivative approach to full creep regions in salt rock", *Mech. Time-Depend. Mater.*, **17**(3), 413-425.

CC